Hindawi
Mathematical Problems in Engineering
Volume 2022, Article ID 2393014, 10 pages
https://doi.org/10.1155/2022/2393014

Research Article

Three-dimensional Face Recognition Method Based on Multiresolution Model and Fuzzy Random Matrix

Ziyou Zhang ,[1,2] Ziliang Feng,[1] Yanqiong Guo ,[1] and Wei Wang [3]

[1] *National Key Laboratory of Fundamental Science on Synthetic Vision, College of Computer Science, Sichuan University, Chengdu, Sichuan 610065, China*
[2] *College of Electronics Information and Artificial Intelligence, Leshan Normal University, Leshan, Sichuan 614000, China*
[3] *School of Control Engineering, Chengdu University of Information Technology, Chengdu, Sichuan 610065, China*

Correspondence should be addressed to Ziyou Zhang; 2017326040007@stu.scu.edu.cn

Received 28 April 2022; Revised 24 May 2022; Accepted 4 June 2022; Published 22 June 2022

Academic Editor: Ning Cao

Three-dimensional face recognition is one of the hotspots of biometric recognition and has a wide range of applications in the fields of information security, video surveillance, video tracking, and so on. The core part of 3D face recognition is to establish the corresponding 3D face model, and the key of building the model is how to obtain the shape model and accurate texture mapping. The problem has not been well solved in the field of face reconstruction. Based on the background, this paper makes an in-depth study and proposes a three-dimensional face recognition method based on multiresolution model and fuzzy random matrix. The face model reconstruction method of image and model can accurately obtain the contour change of face and the representation of specific features through multiresolution model, reduce the inaccurate description of error and noise in samples through fuzzy random matrix, and enhance the effectiveness of image information of classification and recognition. The experimental outcomes exhibit that the 3D face focus approach based totally on multiresolution mannequin and fuzzy random matrix efficiently improves the evaluation effectivity of the model, improves the great of mannequin matching, improves the function extraction in the cognizance process, and improves the attention rate.

1. Introduction

With the development of society and the speedy improvement of laptop technology, in latest years, all components such as visible monitoring, distance education, human-computer interplay technology, automated authentication, and financial institution safety are keen to raise out fast, effective, and secure authentication, particularly in public security, safety authentication system, credit score card authentication, medicine, file management, video conference, human-computer interplay device, and so on [1]. Owing to its steadiness and diversity, biometrics has emerged as the most important skill of authentication. As an herbal body, human face has sturdy commonalities, however due to the impact of person variations and exterior lighting fixtures and different factors, the human face photo has greater complicated sample changes [2]. Compared with exclusive biometrics such as retinal recognition and fingerprint recognition, human face has the features of intuition, friendliness, and convenience. It is attracting extra and greater interest and has a large utility prospect in actual life: face awareness science has emerged as a lookup hotspot in the discipline of sample awareness and synthetic intelligence [3].

Although human beings can effortlessly understand faces and their expressions and can take note and understand heaps of one-of-a-kind faces, computerized desktop cognizance of faces is a very tough task. Compared with the nonrigid object, face cognizance is a greater challenging due to its complicated floor structure [4]. Facial expressions are prosperous and trade with age, the face photograph will alternate extensively due to the modifications of illumination, imaging perspective, and imaging distance. In addition, all faces have similar structural features, and different facial images of the equal character will alternate appreciably due to the alternate of acquisition conditions, so the face attention algorithm wants to mine the refined and reliable versions between one-of-a-kind classes [5, 6]. At the identical time, some algorithms of face attention can be prolonged to the customary three-dimensional (3D) noninflexible object recognition and promote the answer of different sample attention problems. In addition, face attention additionally includes photograph processing, laptop vision, pattern attention and neural network, and is carefully associated to the cognitive degree of human brain, and these elements make face consciousness a very difficult topic [7].

Based on the two-dimensional (2D) mannequin and the 3D model, the matching velocity is noticeably accelerated. In addition, in accordance to the distinction of matching effects underneath specific conditions, the matching outcomes underneath distinctive mindset and illumination prerequisites are in addition analysed. While optimizing the model, blended with the fuzzy random matrix, a higher consciousness impact is achieved. The fuzzy random matrix is used to limit the inaccuracy of the description of the error and noise in the sample and embellish the effectiveness of the photo data of classification and recognition. The experimental penalties show off that the 3D face focal point approach specifically primarily based on multiresolution model and fuzzy random matrix efficaciously improves the assessment effectivity of the mannequin, improves the pleasant of mannequin matching, improves the function extraction in the awareness process, applies different applicable classification applied sciences of synthetic genius to analyse face elements greater effectively, and improves the awareness rate. The organizational shape of this paper is as follows: Section 1 is the introduction, which introduces the applicable background, lookup importance and the foremost work of this paper. Related work is mentioned in Section 2. Section 3 analyses the multiresolution model, fuzzy random matrix, and the matching between 3D face picture and multiresolution model. The scan and evaluation are carried out in Section 4. Section 5 summarizes the full text.

1.1. Related Work. With the growing software of face recognition, many international locations and areas have set up distinct lookup organizations to behaviour in-depth look up on face awareness technology. So far, they have additionally made excellent achievements, and many lookup effects have been utilized to actual life. Relevant research are commonly as follows:

Some students find out about the grasp of face from the standpoint of psychology, learn about the function of intelligence on face recognition, and assemble two useful fashions of face recognition [8, 9]. Others learn about the grasp and cognizance of face from the point of view of physiology or vision. However, most researchers centre their attention on the processing and focus of face images [10]. Scholars have proposed a sparse illustration classifier, SRC technique makes use of the look at picture as the linear sparse illustration of the education samples, obtains the sparsest illustration coefficient via optimizing the norm minimization problem, and then calculates the reconstruction of the look at photo through every kind of coaching samples in accordance to the illustration coefficient to discover the minimal reconstruction error to classify [11]. Like the technique primarily based on sample focus in 2D face recognition, any individual proposed an iterative nearest ordinary factor approach for 3D face recognition. Different from the classical ICP, the proposed approach samples and aligns a set of points, and types the floor everyday vector of the face at the sampling points [12]. The author's conclusion is that the floor everyday vector of the face at the sampling factor carries extra discrimination statistics than the coordinates of the point. Luuk et al. divided the face into more than one overlapping area and fused these areas the use of predominant aspect evaluation linear discriminant analysis [13]. Using 60 fusion place classifiers, the attention fee is improved, and the correlation of adjoining wavelet coefficients is used to overcome the illumination change, which is used to understand 3D face recognition [14].

Like the approach based totally on guide aspects in 2D face recognition, some human beings recommend spherical depth map *(SDM)* to describe the face surface and use uniform down sampling to minimize the range of vertices, to deal with large factor clouds. Elaina et al. [15]. used curved wave characteristic to recognize 3D face recognition. The algorithm detects salient factors on the face and constructs a multiscale neighbourhood floor descriptor to achieve nearby points that are invariant to rotation and displacement [16]. The 3D face picture is divided into inflexible and semirigid regions, and four nearby geometric histogram aspects are extracted. Finally, guide vector laptop (*SVM*) is used to classify features, and unique classes correspond to special individuals [17]. Experiments exhibit that the fusion of inflexible and semirigid regional facets can grant a dependable foundation for facial expression changes. SIFT elements are used to hit upon and in shape spatial extremum on six extraordinary scales. This approach is sturdy to noise and expression changes.

2. Related Theories and Technologies

2.1. Face Recognition Theory. As the unique photograph records gathered using the machine will be affected via many factors, it is now not handy to immediately elevate out function extraction and different work, so the accrued photographs must be preprocessed. Image preprocessing refers to the processing of the bought facial photo information, such as colour transformation, geometric transformation, and Gray transformation [18]. Only by acquiring the perfect face picture can we lay a stable basis for extracting advantageous characteristic information.

As most of the photographs gathered in realistic purposes are colour and the present face focus applied sciences are primarily based on Gray picture research, the first work is to convert the colour photograph into Gray image. Grayscale photographs solely include depth data and do no longer incorporate colour information [19]. They are generally represented by means of a matrix. The values in the matrix symbolize exceptional grayscale. Colour photographs are composed of three colours: pink (R), inexperienced (G), and blue (B), which can be modified into grayscale photographs through brightness operation. Unify the geometric dimension of the image, that is, normalize all pictures by using geometric transformation [20]. Geometric transformation does now not radically change the photograph pixel value, which usually consists of two parts: photograph scaling processing and deciding the geometric transformation algorithm. Gray interpolation algorithm is chosen to clear up the hassle that pixels are mapped to noninteger coordinates after photo scaling [21].

In this paper, all snap shots are scaled to a unified size, and bilinear interpolation algorithm is used to keep away from mosaic impact brought about by way of scaling images. After the coloration transformation and geometric transformation of facial image, it is additionally vital to trade its Gray degree and standardize its Gray level [22]. It is in most cases composed of histogram equalization and Gray normalization. The operation of histogram equalization is a factor operation, which adjusts the Gray price of the photo factor by way of point and tries to make every Gray stage have the equal range of pixels to make the histogram tend to balance. Histogram equalization can convert the entire photograph into an output photograph with the identical variety of pixels at every Gray level [23]. The method of equalization is as follows: relay the histogram of the photo to be processed and calculate its distribution function. According to the statistical histogram, the cumulative distribution feature is used for transformation to acquire the new Gray degree after transformation. The new Gray stage is used to change the historical Gray level, and the distribution characteristic of the new Gray stage is obtained. At the identical time, the Gray values are equal or about combined. Basic process of face recognition is shown in Figure 1.

2.2. 3D Multiresolution Face Model. By uniformly resampling one-of-a-kind faces, the alignment outcomes at special resolutions can be obtained. On this basis, a multiresolution 3D deformation mannequin is established. This mannequin can no longer solely in accordance to countless 2D images, however additionally at once, alter the deformation coefficient to deform exceptional 3D faces [24]. In addition to the aforementioned alignment work, the trouble to be viewed in the system of organising the mannequin is the diploma of face deformation. It is critical to make certain the authenticity of the result of face deformation, that is, to make sure the actual 3D face [25].

According to the 3D model, alter the deformation coefficient of face structure and texture to get specific faces. New faces and expressions can be received by means of linear aggregate of exclusive prototype faces [26]. The chance distribution characteristic is acquired from the distribution evaluation of form and texture. According to the chance distribution function, the diploma of face deformation is limited. Using the model, the 2D face picture can be analysed to reap the 3D structure of the face, and the 3D face with extraordinary results can additionally be acquired with the aid of manually adjusting the deformation coefficient. Sampling regeneration process based on multiresolution is shown in Figure 2.

The traits of 3D multiresolution deformation mannequin frequently lie in two aspects: one is multiresolution, that is, the diploma of sampling leads to the deformation mannequin in the case of multiresolution [27]. On the contrary, it is the deformation traits of the model, which includes the alternate of contour and the characterization of features. The key to constructing the mannequin is the alignment of 3D face. According to the above 3D face alignment algorithm based totally on resampling technology, the 3D faces chosen from the library as the foundation of modelling are resampled uniformly, and the resampling effects of every 3D face at unique resolutions are recorded [28].

The 3D multiresolution mannequin is based totally on the 3D face database. When all faces are aligned, mutual deformation operations can be executed between distinctive faces. In the aforementioned work, exclusive faces have been aligned at five resolutions. We characterize the 3D face aligned underneath distinctive resolutions as follows, and the structure vector is expressed as follows:

$$S = (X_1, Y_1, Z_1, \ldots, X_n, Y_n, Z_n)^T. \tag{1}$$

x, y, and z represent the 3D coordinate values of n points, while RLT represents the sequence number of the current resolution, $RLT = 1, 2, 3, 4, 5$. Similarly, the texture information of different points can also be represented by vectors, which are as follows:

$$T^{\text{rlt}} = (R_1, G_1, B_1, \ldots, R_n, G_n, B_n)^T. \tag{2}$$

R, G, and B represent the colour values of the aforementioned n points. Use already aligned each face can be represented by its shape vector T^{rlt} and texture vector S^{rlt}. Owing to the alignment under different resolutions, the new 3D face can be represented as follows:

$$S^{\text{rlt}} = \frac{\sum_{i=1}^{m} a_i S_i^{\text{rlt}}}{a_i + S_i} + \frac{\lambda_i}{n}, T^{\text{rlt}} = \frac{\sum_{i=1}^{m} b_i T_i^{\text{rlt}}}{b_i + T_i} + \frac{\lambda_i}{n}, \tag{3}$$

It should be emphasized that there is correlation between 3D points under different resolutions, and the value of deformation parameter a_i, b_i is the same under different resolutions. In this way, the 3D multiresolution deformation model can be defined as a 3D representation, the deformation of the model to 3D faces with different shapes and textures can be controlled [29].

For a truly effective face synthesis system, there should be a specific measure of the authenticity of the synthetic face. Therefore, we make an overall probability analysis of the deformation parameter a_i, b_i of 3D face in the database. According to the estimated probability distribution, the authenticity of the generated face can be summarized by analysing the current value of a_i, b_i. We analyse 200 3D face objects selected from the library according to the calculated average shape S^{rlt} and texture T^{rlt}. In the case of the highest resolution, that is, $RLT = 5$, to further calculate the final shape and texture in the case of the highest resolution.

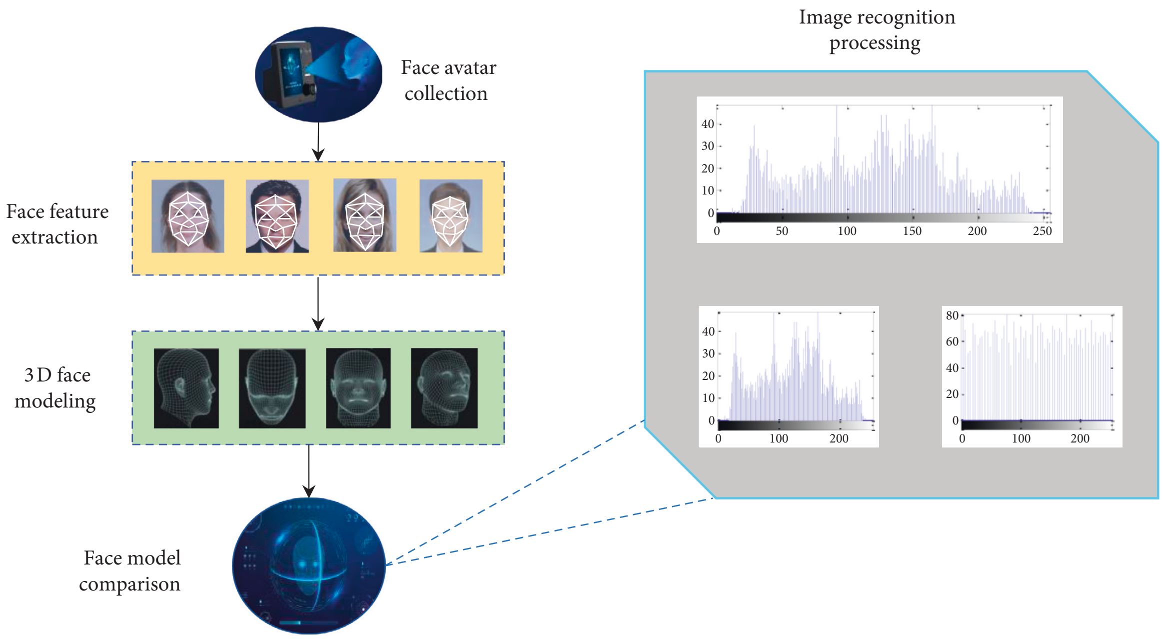

Figure 1: Basic process of face recognition.

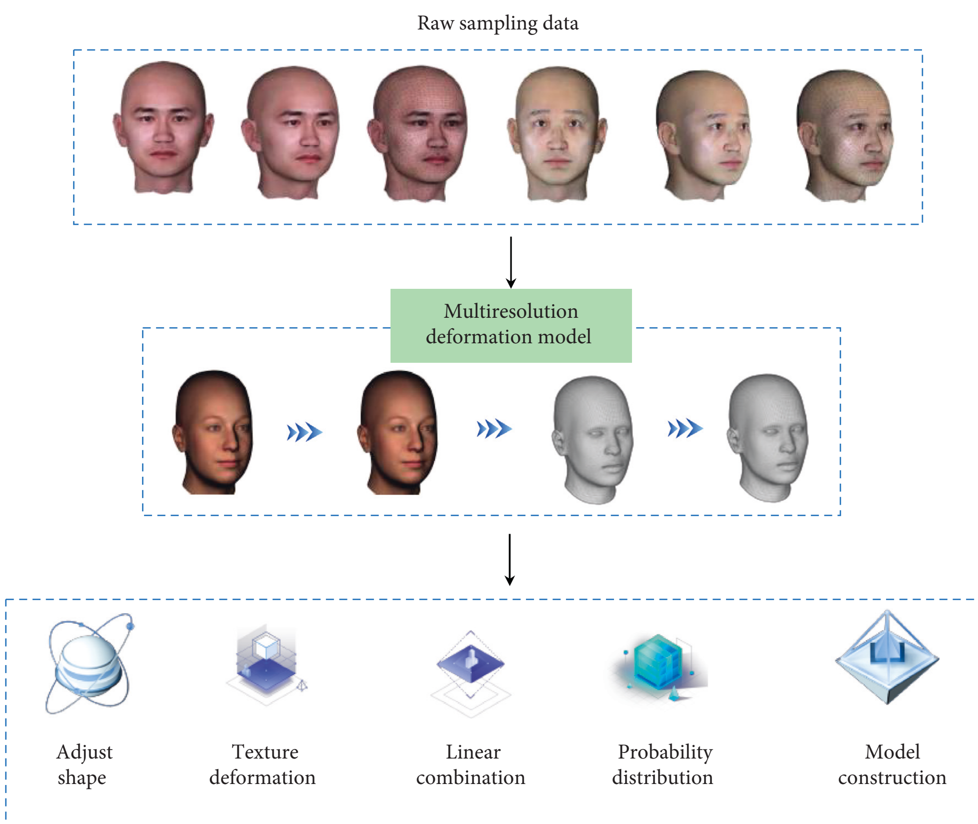

Figure 2: Sampling regeneration process based on multiresolution.

2.3. Matching of Face Image and 3D Multiresolution Model. The key to constructing the mannequin is the point-to-point alignment of 3D faces in the database. According to the structure similarity of 3D faces, we endorse a new approach primarily based on 3D facts resampling. All 3D faces are segmented and resampled uniformly to attain a 3D face database with the equal topology. Based on this database, the important thing evaluation technique can be without difficulty used to set up the mannequin. The following briefly introduces the software program of resampling in 3D face alignment. For all prototype face data, the machine is used for unified segmentation, and each and every face will be divided into endless related flake areas [30]. The area is similarly subdivided, and the uniform sampling grid is bought in accordance to the function of the elastic factors adjusted via the resultant pressure of the factors. After uniformly resampling every face, the unified topology of all 3D faces is obtained, and a whole alignment relationship is established. On this basis, 3D face fashions below distinct resolutions are installed in accordance to the variety of subdivision times.

The basis of 3D face deformation model is established under different resolution conditions, the model can be expressed as follows:

$$S^{\mathrm{rlt}} = \frac{\sum_{j=1}^{m} \alpha_i S_j^{\mathrm{rlt}}}{\alpha_i + S_i} + \frac{\lambda_i}{n}, T^{\mathrm{rlt}} = \frac{\sum_{i=1}^{m} \beta_i T_i^{\mathrm{rlt}}}{\beta_i + T_i} + \frac{\lambda_i}{n}. \tag{4}$$

The superscript *RLT* represents the resolution, $S^{\mathrm{rlt}}, T^{\mathrm{rlt}}$ respectively represent the shape and texture value of each face in the library under different resolutions, and the shape and texture deformation coefficient α_j, β_j has the same value under different resolutions in order to represent 3D faces; principal component analysis is performed more effectively on S_j^{rlt} and T_j^{rlt} respectively to eliminate the correlation between different faces:

$$\begin{aligned} S^{\mathrm{rlt}} &= \frac{S_{\mathrm{avg}} + \sum_{i=1}^{m} \alpha_i S_i^{\mathrm{rlt}}/\alpha_i + S_i + \lambda_i/n}{\alpha_i}, \\ T^{\mathrm{rlt}} &= \frac{T_{\mathrm{avg}} + \sum_{i=1}^{m} \beta_i T_i^{\mathrm{rlt}}/\beta_i + T_i + \lambda_i/n,}{\beta_i}. \end{aligned} \tag{5}$$

In the formula, S_{avg} and T_{avg} are the eigenvectors of S_j^{rlt} and T_j^{rlt} covariance matrices, at the same time, we can also get α and β priori probability.

$$\begin{aligned} \zeta(\alpha) &= \frac{\exp\left[\sum_{i=1}^{m} \alpha_i S_i^{\mathrm{rlt}}/\alpha_i + S_i\right] + \lambda_i/n}{\alpha_i}, \\ \zeta(\beta) &= \frac{\exp\left[\sum_{i=1}^{m} \beta_i S_i^{\mathrm{rlt}}/\beta_i + S_i\right] + \lambda_i/n}{\beta_i}. \end{aligned} \tag{6}$$

According to the resolution from low to high, the face image is matched with the 3D multiresolution model. The model deformation coefficient calculated at low resolution is used as the initial value of the deformation coefficient at higher resolution. The final coefficient is analysed to achieve the purpose of recognition. The goal of image and model matching is to obtain the model deformation coefficient $\alpha_i, \beta_i, \quad i = 1, 2, \ldots, n$ and external condition parameters ρ, it includes the corresponding number and position of light sources, illumination intensity, face pose and other information [31]. The mannequin can be projected onto 2D via the use of snap shots approach to make the generated photograph as identical as the entire picture as viable. Some different parameters, such as digital camera role and face floor material, want to be given a constant value [32]. Under the condition of different resolutions, in order to deform the 3D model into the similar face in the input image, it is necessary to continuously reduce the difference between the synthetic image and the input image, which can be expressed as follows:

$$E^{\mathrm{rlt}} = \frac{\sum_{x,y} \left\| I_{44}(x, y) - I_{\mathrm{input}}(x, y) \right\|^2}{\sqrt{x^2 + y^2}}. \tag{7}$$

Here, the value of $I_{\mathrm{input}}(x, y)$ can be obtained through the coordinate transformation from 3D to 2D, and the input relative to a, b can be obtained by analysing the phung illumination model, ρ given a standard deviation σ_N^{rlt}, the posterior probability of can be expressed as follows:

$$p\left(I_{\mathrm{input}} \mid \alpha, \beta, \rho\right) = \frac{E^{\mathrm{rlt}}}{2\left(\sigma^{\mathrm{rlt}}\right)^2} + \exp\left(\frac{\alpha_i}{\alpha_i + \beta_i + \rho_i}\right). \tag{8}$$

The maximum a posteriori probability method is used to minimize at different resolutions. Take the initial value of ρ_i as $\bar{\rho}_i$, take a specific value for $\sigma_{\rho,i}$, and get the a priori probability representation of ρ_i hypothesis α and β Independent of each other, combined with formula (4), put a, β, ρ, the product of a priori probability is taken as at this time, the aforementioned E^{rlt} can be transformed into:

$$E^{\mathrm{rlt}} = \frac{E^{\mathrm{rlt}}/\left(\sigma_N^{\mathrm{rlt}}\right)^2 + \sum_i \alpha_i^2/\left(\sigma_N^{\mathrm{rlt}}\right)^2}{\sum_i \beta_i^2/\left(\sigma_N^{\mathrm{rlt}}\right)^2 + \sum_i\left(\rho_i - \bar{\rho}_i\right)^2}. \tag{9}$$

According to the random gradient descent method, in each iteration, several triangular surfaces are randomly selected from the model with current resolution, E^{rlt} is calculated for the centre point of each surface, and then the gradient of each parameter is calculated and the corresponding parameters are changed respectively [33]. In order to make the randomly selected triangular surface better reflect the overall change, the gradient change is affected according to the proportion of the projected area of each surface to the sum of the projected areas of all random surfaces. Before the iteration, calculate the area of all faces once, and then calculate the area every 1000 steps of the iteration, and discard those blocked faces according to the projection of the face In addition, the first few iterations are to take a larger value for σ_N^{rlt}. After optimizing only, the first few coefficients $\alpha_i, \beta_i, \quad i = 1, 2, \ldots, 10$ and all ρ_i, the optimized σ_N^{rlt} increases gradually as the value of α_i, β_i decreases for the database of 200 faces, there are up to 199 coefficients α_i, β_i for principal component analysis. Here, only the most useful components with the largest eigenvalues of the first 99 are taken, so as to form the shape and texture vector with 99 components α, β. When the optimization reaches a certain degree under the current resolution conditions, the α, β, ρ value as the initial value in the model matching of higher resolution, and then continue to optimize according to the aforementioned steps under the condition of this resolution α, β, ρ, until b reaches a certain threshold. Because there are few triangles in the model under the condition of low resolution and the amount of calculation is small when considering the whole, the multiresolution model greatly speeds up the matching speed [34, 35].

3. Results and Analysis

In order to consider the overall performance of 3D face consciousness approach primarily based on multi-resolution mannequin and fuzzy random matrix, experiments are carried out on more than one face databases, which are divided into four parts: illumination and expression exchange experiments, which are carried out on *AR* and prolonged *Yale B* face databases; Attitude deflection scan is carried out on *ORL* face database; Camouflage experiment, carried out on *AR* face database. The noise trade test was once carried out on the prolonged *Yale B* face database.

3.1. Experiment of Expression Change under Light. In this crew of experiments, 14 unobstructed snap shots of every kind of pattern are selected, the first seven snap shots of every kind of sample, a complete of 882 images, are chosen as the education pattern set, and the relaxation are used as the check pattern set. In the education stage, three snap shots of every kind of pattern are chosen for the calculation of weight vector. Owing to the giant dimension of the extracted function vector, *PCA* is used to decrease the dimension and then *SRC* consciousness is carried out. The consciousness prices of a range of algorithms beneath distinct function dimensions are compared. A whole of 20 experiments had been taken and their imply values had been recorded. The experimental consequences are proven in Figure 3.

Three photos of every kind of pattern are used to calculate the weight vector w, and set two is chosen as the check pattern set. In the experiment, the characteristic dimension is decreased to one hundred dimensions, and the attention charges of this algorithm and the different three algorithms are in contrast beneath exceptional illumination changes. The effects are proven in Figure 4.

It can be considered from Figures 3 and 4 that the algorithm in this paper can acquire the nice consciousness impact below unique illumination and expression changes. With the deterioration of illumination conditions, the consciousness rate of the extraordinary three single-feature algorithms decreases rapidly, alternatively the algorithm in this paper can on the other hand preserve the attention fee of 73.42% when the illumination changes violently.

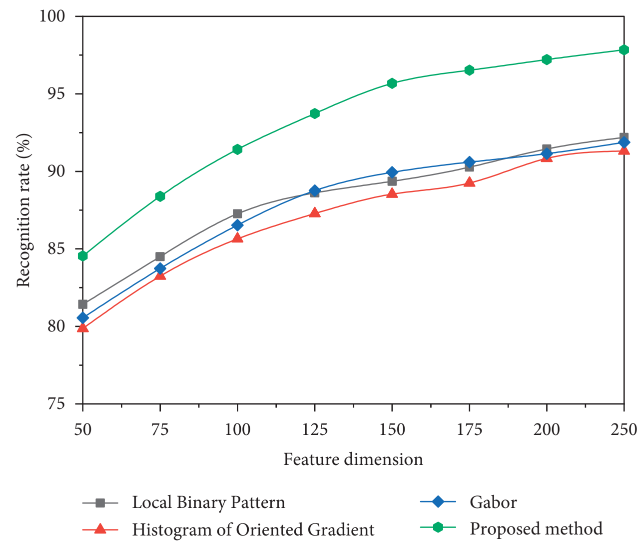

Figure 3: Comparison of recognition rates of different methods on AR face database.

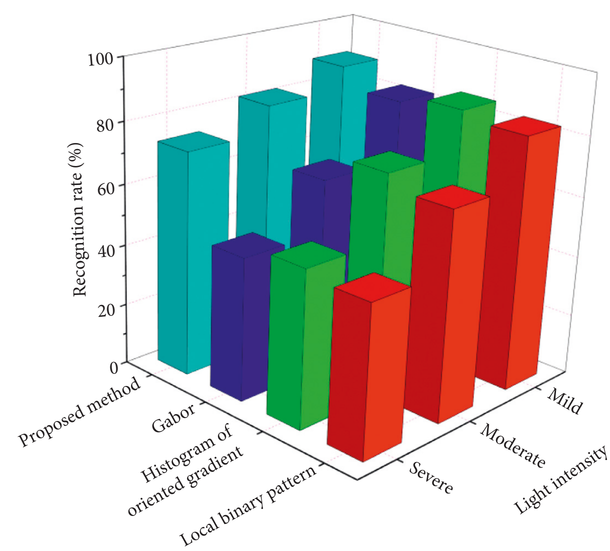

Figure 4: Comparison of recognition rate under different illumination conditions.

3.2. Attitude Deflection Experiment. Select the first 5 face pictures of every kind as coaching samples and the relaxation as look at samples, and pick out three snap shots of every kind of samples from the coaching samples for the calculation of weight vector w. Experiments are carried out on every algorithm when the function dimensions are 50, 75, 100, 125, 150, 175, 200, and 250, and the awareness price is compared. Twenty experiments are carried out, and the common fee is recorded. The effects are recorded in Figure 5.

As can be viewed from Figure 5, when the pattern picture has mindset deflection, the *LBP* characteristic awareness impact is the first-class amongst the three single-function awareness algorithms. Under specific characteristic dimensions, the focus impact of this algorithm is substantially higher than the single characteristic cognizance algorithm, and the attention fee is 5% greater than the different three single-function awareness algorithms.

3.3. Camouflage Occlusion Experiment. In the experiment, 14 unobstructed snap shots of every kind of humans are chosen as the coaching pattern set, the final 12 occluded pictures are used as the check pattern set, and 5 photographs of every kind of samples are chosen from the education samples for the calculation of weight vector w. Experiment and examine the consciousness fee of every algorithm when the function dimension is 50, 75, 100, 125, 150, 175, 200, and 250. A whole of 20 experiments is carried out and the common fee is recorded. The outcomes are recorded in Figure 6.

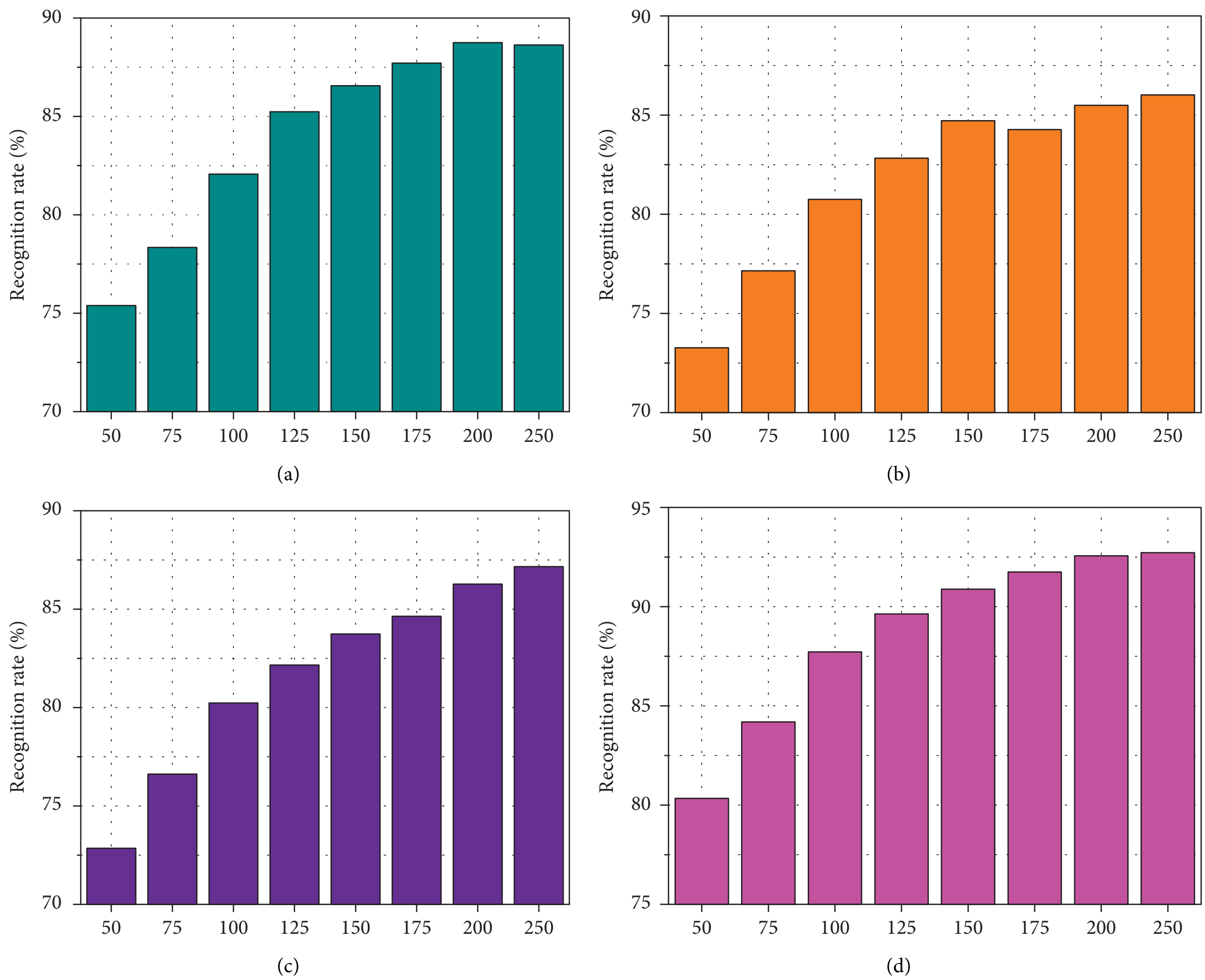

FIGURE 5: Comparison of recognition rates of different methods on ORL face database: (a) local binary pattern, (b) histogram of oriented gradient, (c) gabor, and (d) proposed method.

3.4. Noise Change Experiment. In the experiment, five pix of every kind of pattern are chosen from the education samples for the calculation of weight vector w, and the dimension of every characteristic vector is set to 150 dimensions. A whole of 20 experiments is carried out, and the common price is recorded. Figure 7 showed the information the focus effects of every algorithm when including noise ratios of 20, 25, 30, 35, 40, 45, 50, 55, and 60 to the check samples. The recognition rates of different methods vary with the degree of noise pollution.

From the above results, the focus price of this algorithm decreases exceptionally slowly when the pattern is polluted by using noise, and it nevertheless reaches 68.25% when the air pollution share reaches 60%. Among the three single-function attention algorithms, Gabor function has the strongest antinoise capability and *LBP* characteristic is the weakest. Through exceptional experiments on a couple of face databases, the consciousness charge of the proposed algorithm is greater than that of the three single features. Because the algorithm proposed in this paper is well suited with the benefits of *LBP*, hog and Gabor algorithms: *LBP* steady mode can higher signify the element statistics of adjoining pattern areas of pattern images, and the acquired characteristic data are extra complete and effective. The hog function can preserve right invariance to the geometric or optical deformation of the pattern image; Gabor wavelet seriously changes and can extract the frequency area elements of nearby pattern pix in multidirectional and multiscale space. Therefore, the algorithm combining the three facets has higher awareness impact than a single feature.

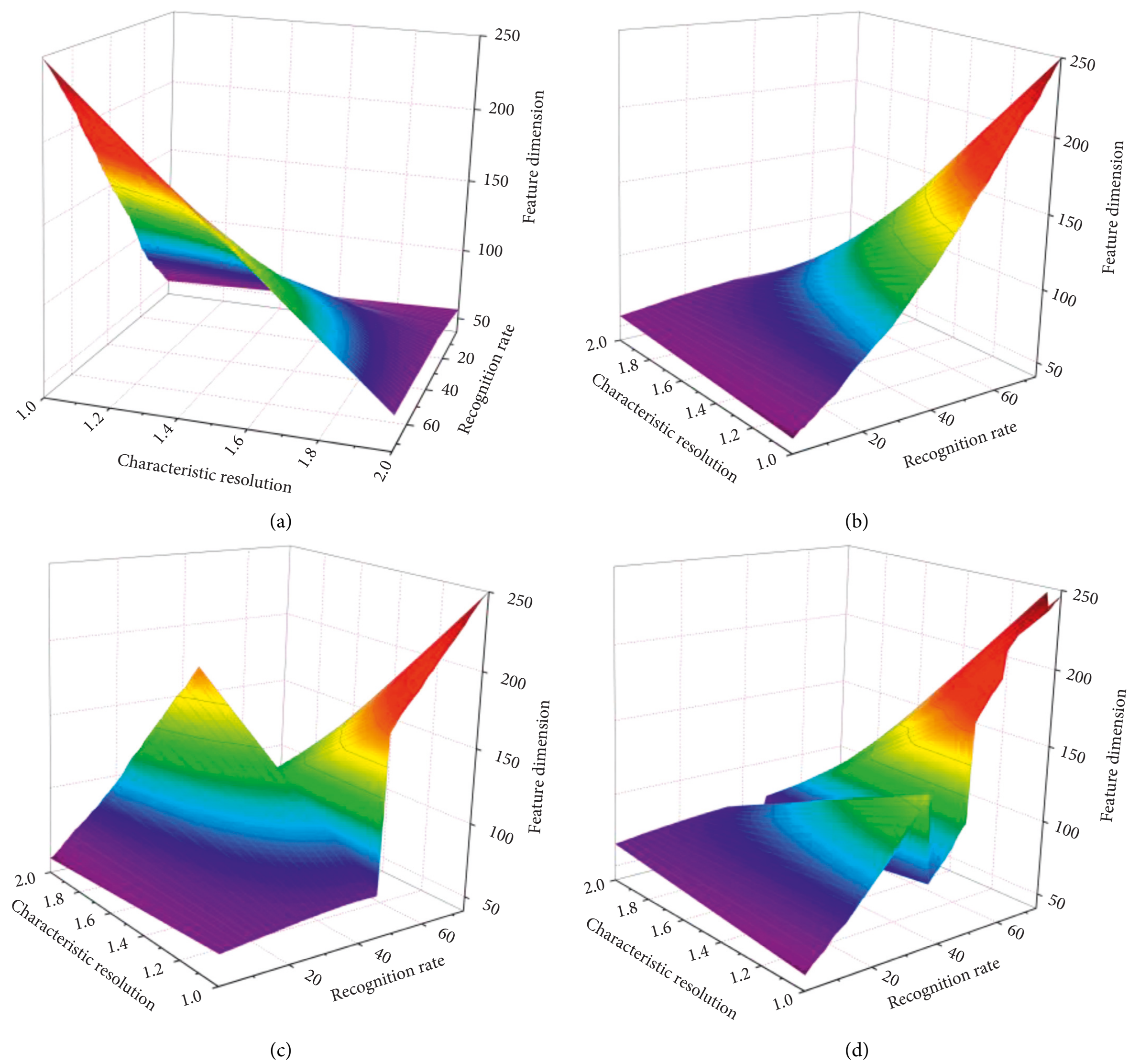

Figure 6: Comparison of recognition rates of different methods under camouflage and occlusion: (a) local binary pattern, (b) histogram of oriented gradient, (c) gabor, and (d) proposed method.

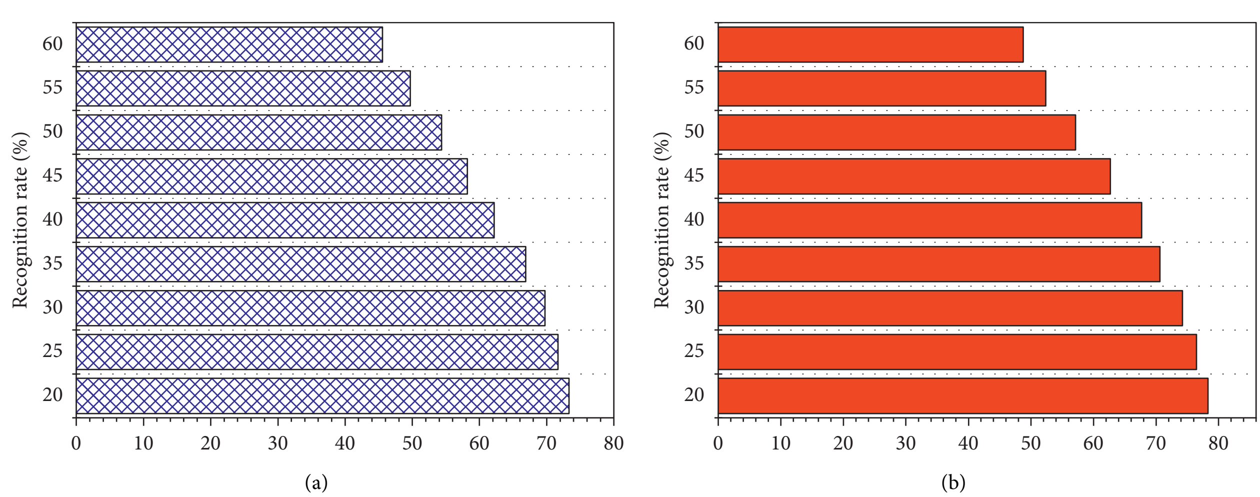

Figure 7: Continued.

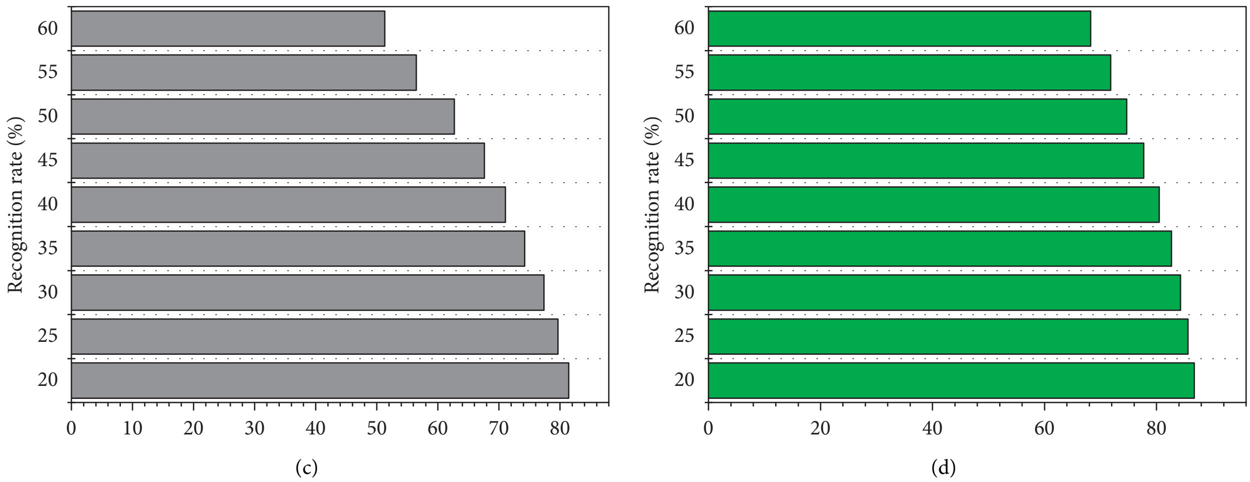

FIGURE 7: The change of recognition rate of different methods with the degree of noise pollution: (a) local binary pattern, (b) histogram of oriented gradient, (c) gabor, and (d) proposed method.

4. Conclusion

This paper gives a 3D face consciousness technique primarily based on multiresolution mannequin and fuzzy random matrix, discusses in element the new algorithm proposed in this paper to fuse the reconstructed residuals underneath extraordinary features, and verifies the effectiveness and feasibility of the proposed technique in a couple of face databases. This paper focuses on the low rank restoration sparse illustration face awareness algorithm based totally on characteristic fusion, and proposes a characteristic fusion technique that makes use of the nearby classification outcomes and classification residuals to assemble the loss function, and makes use of the least rectangular approach and regularization to remedy the most useful weight vector. Then, beneath the unified experimental environment, the consciousness consequences of three single-function cognizance algorithms and characteristic fusion algorithms are analysed and in contrast to verify the effectiveness of the algorithm proposed in this paper. Especially in the case of uneven illumination, expression change, mindset deflection and noise air pollution in the face image, the algorithm is extra robust. In the gadget of face recognition notably primarily based on 3D model, the enchantment of the aforementioned alignment will straight away have an impact on the contrast effectivity of the model and improve the quality of model matching and feature extraction in the technique of recognition. In the diagram of classifier, we can enlarge the kinds and elements of face snap shots in Fisher coaching database and reflect on consideration on the usage of different applicable classification applied sciences of synthetic genius to analyse face points greater efficiently and enhance the consciousness rate.

Data Availability

The data used to support the findings of this study are available from the corresponding author upon request.

Conflicts of Interest

The authors declare that they have no conflicts of interest or personal relationships that could have appeared to influence the work reported in this paper.

Acknowledgments

This work was supported by the National Key Laboratory of Fundamental Science on Synthetic Vision, College of Computer Science, Sichuan University.

References

[1] H. Q. He, J. Q. Yan, and K. H. Hui, "Lightweight face recognition method based on deep residual network," *Computer Applications*, vol. 12, no. 7, pp. 1–8, 2021.

[2] X. Liu, "Face enhancement recognition method based on deep learning in low quality video," *Computer Knowledge and Technology*, vol. 17, no. 22, pp. 94–96, 2021.

[3] Q. Q. Pei, "Research on face recognition method based on deep learning algorithm," *Electronic Technology and Software Engineering*, vol. 18, no. 6, pp. 114-115, 2021.

[4] G. Cattle and C. Wen, "Face recognition method combining feature enhancement and network parameter optimization," *Information and Control*, vol. 50, no. 3, pp. 350–355, 2021.

[5] Y. Chen and K. N. Y. G. Lee, *Acta Biomaterialia*, vol. 114, no. 23, pp. 158–169, 2020.

[6] Z. L. Ren and X. G. Xue, "Face recognition based on deep learning," *Control Engineering*, vol. 29, no. 4, pp. 738–742, 2022.

[7] Z. J. Sui, "Application of sparse projection in face recognition," *Electronic Technology and Software Engineering*, vol. 16, no. 6, pp. 147-148, 2020.

[8] T. Fang, J. Yang, L. Liu, and H. X. Xiao, *MedComm*, vol. 2, no. 2, pp. 279–287, 2021.

[9] P. C. Yan, Y. M. Zhang, G. H. Tong, F. Huang, and X. F. Ou, "Video surveillance face recognition method based on convolutional neural network," *Journal of Chengdu Institute of Technology*, vol. 23, no. 1, pp. 26–31, 2020.

[10] M. Wang, "Face recognition method based on deep learning," *Computer and Digital Engineering*, vol. 48, no. 2, pp. 433–435, 2020.
[11] Y. J. Huang, J. Zuo, and B. J. Sun, "Research progress of face recognition methods based on deep learning," *Modern Computer*, vol. 24, no. 7, pp. 67–71, 2020.
[12] J. Hu, Y. Tao, T. Guo, Y. H. Sun, H. Hu, and J. Wang, "Group sparse representation face recognition method based on low rank matrix restoration," *Computer Engineering and Design*, vol. 40, no. 12, pp. 3588–3593, 2019.
[13] C. Yang, C. Li, J. Sun, and X. Lu, "Role of estradiol in mediation of etomidate-caused seizure-like activity in neonatal rats," *International Journal of Developmental Neuroscience*, vol. 78, no. 1, pp. 170–177, 2019.
[14] G. Betta, D. Capriglione, M. Corvino, and A. C. P. E. Lavatelli, "Metrological characterization of 3D biometric face recognition systems in actual operating conditions," *Acta Imeko*, vol. 6, no. 1, p. 33, 2017.
[15] L. Spreeuwers, "Breaking the 99% barrier: optimisation of three-dimensional face recognition," *IET Biometrics*, vol. 4, no. 3, pp. 169–178, 2015.
[16] S. Ouyang, T. Hospedales, Y.-Z. Song, and X. C. C. X. Li, "A survey on heterogeneous face recognition: sketch, infra-red, 3D and low-resolution," *Image and Vision Computing*, vol. 56, no. 12, pp. 28–48, 2016.
[17] T. Liu, "Face recognition method based on local feature analysis," *Information and Computer (Theoretical Edition)*, vol. 31, no. 21, pp. 114-115, 2019.
[18] R. Gong, S. Ding, C. H. Zhang, and H. Su, "Lightweight and multi pose face recognition method based on deep learning," *Computer Applications*, vol. 40, no. 3, pp. 704–709, 2020.
[19] Y. Shen and S. G. Y. Z. Z. Q. Zhang, *Journal of interventional medicine*, vol. 2, no. 4, pp. 154–159, 2019.
[20] M. R. Peng, "Face recognition method based on nonnegative matrix decomposition algorithm," *Journal of Changchun Institute of Engineering*, vol. 20, no. 3, pp. 104–108, 2019.
[21] C. F. Du, Y. L. Wen, and J. Z. Li, "Multi state adaptive face recognition method based on deep convolution countermeasure neural network," *Mobile Communications*, vol. 43, no. 9, pp. 75–78, 2019.
[22] Y. Qin and H. Xiao, "Research on face recognition method based on adaptive nonnegative matrix decomposition," *Software Guide*, vol. 18, no. 12, pp. 73–77, 2019.
[23] W. M. Xu, P. Zhang, and S. Q. Wu, "Robust face recognition method based on sparse representation of multi-directional Gabor feature map," *Journal of Beijing University of Technology*, vol. 39, no. 7, pp. 732–737, 2019.
[24] X. H. Lu, L. F. Wang, S. H. Zeng, and J. J. Chen, "Multi pose face image recognition algorithm based on neural network learning," *Computer Technology and Development*, vol. 29, no. 11, pp. 57–61, 2019.
[25] S. C. Hu, "Research on face recognition method based on deep learning," *Electronic Technology*, vol. 32, no. 6, pp. 82–86, 2019.
[26] L. H. Huang, Z. C. Kang, C. F. Zhang, and T. Cheng, "Face recognition method based on lightweight convolutional neural network," *Journal of Hunan University of technology*, vol. 33, no. 2, pp. 43–47, 2019.
[27] M. D. Wu, "Research on 3D face recognition method based on deep learning," *Shandong Industrial Technology*, vol. 18, no. 22, pp. 156-157, 2019.
[28] G. L. Sang, Z. G. Zheng, and C. Yan, "Expression robust 3D face recognition method based on region segmentation," *Computer Application Research*, vol. 37, no. 3, pp. 914–918, 2020.
[29] Y. Bu, J. X. Liu, and W. D. Chen, "3D face recognition method based on coordinate system face registration and integrated classifier," *Journal of Southwest Normal University (Natural Science Edition)*, vol. 42, no. 10, pp. 106–114, 2017.
[30] X. Yuan, Z. H. Wang, and W. T. Jiang, "3D face recognition method based on singular point neighborhood structure," *Control and Decision Making*, vol. 32, no. 10, pp. 1739–1748, 2017.
[31] J. T. Wang, L. Zhao, and X. B. Qi, "Face recognition method based on adaptive 3D deformation model combined with manifold analysis," *Computer Science*, vol. 44, no. 17, pp. 232–235, 2017.
[32] Z. X. Chen and D. K. Zhou, "Huang Jingwei Expression invariant 3D face recognition based on convolutional neural network," *Electronic Measurement Technology*, vol. 40, no. 4, pp. 157–161, 2017.
[33] M. Huang, Q. P. Gong, and S. Zeng, "3D face recognition based on depth data," *Journal of Zhengzhou Institute of Light Industry*, vol. 29, no. 6, pp. 78–80, 2014.
[34] N. I. Ratyal, I. A. Taj, U. I. Bajwa, and M. Sajid, "3D face recognition based on pose and expression invariant alignment," *Computers & Electrical Engineering*, vol. 46, no. 13, pp. 241–255, 2015.
[35] T. Napoléon and A. Alfalou, "Pose invariant face recognition: 3D model from single photo," *Optics and Lasers in Engineering*, vol. 89, no. 4, pp. 150–161, 2017.